Effects of industrially produced 2-dimensional molybdenum disulfide materials in primary human basophils

Hazel Lin, Antonio Esau del Rio Castillo, Viviana Jehová González, Lucas Jacquemin, Jaya Kumar Panda, Francesco Bonaccorso, Ester Vázquez, Alberto Bianco

NanoImpact 29 (2023) 100451

Contents lists available at ScienceDirect

NanoImpact

journal homepage: www.elsevier.com/locate/nanoimpact

Effects of industrially produced 2-dimensional molybdenum disulfide materials in primary human basophils

Hazel Lin [a], Antonio Esau del Rio Castillo [b], Viviana Jehová González [c], Lucas Jacquemin [a], Jaya Kumar Panda [b], Francesco Bonaccorso [b], Ester Vázquez [c], Alberto Bianco [a,*]

[a] CNRS, Immunology, Immunopathology and Therapeutic Chemistry, UPR 3572, University of Strasbourg, ISIS, Strasbourg 67000, France
[b] BeDimensional, Lungo Torrente Secca 30r, Genoa, Italy
[c] Biograph Solutions, Regional Institute of Applied Scientific Research (IRICA), Department of Organic Chemistry, Faculty of Science and Chemistry Technologies, University of Castilla-La Mancha, Ciudad Real 13071, Spain

ARTICLE INFO

Editor: Bernd Nowack

Keywords:
Immune system
Toxicity
Industrial 2D nanomaterial
Molybdenum
Cell activation

ABSTRACT

MoS_2 has been increasingly used in place of graphene as a flexible and multifunctional 2D material in many biomedical applications such as cancer detection and drug delivery, which makes it crucial to evaluate downstream compatibility in human immune cells. Molybdenum is a component of stainless-steel stent implants and has previously been implicated in stent hypersensitivity. In view of this, it is important to ascertain the effect of MoS_2 on allergy-relevant cells. Basophils are a less commonly used immune cell type. Unlike mast cells, basophils can be easily derived from primary human blood and can act as a sentinel for allergy. However, merely testing any one type of MoS_2 in basophils could result in different biological results. We thus decided to compare 2D MoS_2 from the two companies BeDimensional© (BD) and Biograph Solutions (BS), manufactured with two different but commonly exploited methods (BD, deoxycholate surfactant in a high-pressure liquid exfoliation, and BS using glycine in ball-milling exfoliation) to elucidate immunological end-points common to both MoS_2 and to demonstrate the need for biological verification for end-users who may require a change of supplier. We report higher histamine production in human basophils with MoS_2. No effects on either surface basophil activation markers CD63 and CD203c or reactive oxygen species (ROS) production and cell viability were observed. However, different cytokine production patterns were evidenced. IL-6 and IL-1β but not TNF and GM-CSF were increased for both MoS_2. BS-MoS_2 increased IL-4, while BD-MoS_2 decreased IL-4 and increased IL-13. Molybdate ion itself only increased IL-1β and IL-4. Deoxycholate surfactant decreased viability at 18 h and increased ROS upon basophil activation. Therefore, these results demonstrate the safety of MoS_2 in human basophils in general and highlight the importance of considering manufacturer additives and variability when selecting and investigating 2D materials such as MoS_2.

1. Introduction

Molybdenum is found in the environment in molybdenite form (MoS_2) and in all plants and animals as an enzyme co-factor. It can also be released from mining activities (ATSDR, 2017). Molybdenum has been used in various industries to make alloys, lubricants, chemicals and electronics due to its high thermal conductivity and low coefficient of thermal expansion, which enable it to enhance material strength, weldability and corrosion resistance (IMA, 2008).

Molybdenum exists in different oxidation states, and MoS_2 (Mo IV) can be oxidized into water-soluble molybdate species (Mo VI). Although the synthetic MoS_2 is becoming one of the most investigated forms in recent years, being the following most commonly researched 2D material after graphene (Li and Zhu, 2015; Capasso et al., 2016), its *in vitro* effects in specific cells remain unknown. Like most 2D transition metal dichalcogenides, MoS_2 has unsaturated edge coordination, a high surface-volume ratio, and electronic structures that range from metallic, semi-metallic to semiconducting, depending on their crystal phase (Najafi et al., 2017; Han et al., 2018). These physical characteristics make it suitable for various uses. Particularly in biomedicine, MoS_2 has been used for miRNA detection (Ge et al., 2020), cancer peroxide sensing (Hu et al., 2020) and drug delivery (Zhao et al., 2019). Of note,

* Corresponding author.
E-mail address: a.bianco@ibmc-cnrs.unistra.fr (A. Bianco).

https://doi.org/10.1016/j.impact.2023.100451
Received 3 November 2022; Received in revised form 28 December 2022; Accepted 4 January 2023
Available online 7 January 2023

MoS_2 is less toxic than graphene and its analogues (Teo et al., 2014), and has no long-term persistence in living systems, (Kurapati et al., 2017a), making it more biocompatible for physiological applications. However, molybdenum hypersensitivity *via* released molybdate ions in stainless steel stents has been implicated in restenosis in coronary artery stent patients (Köster et al., 2000) and metal plate implants (Federmann et al., 1994). Nanomaterial-derived molybdenum has also been reported to affect physiological molybdenum enzymes by elemental incorporation (Cao et al., 2021). The molybdenum release makes it essential to validate MoS_2 safety and propensity for causing allergy, given its high potential to be incorporated into implants or other biomedical devices.

The impact of 2D materials on immune cells has been primarily investigated in macrophages, the main phagocytic cells (Lin et al., 2021). However, it is important to ascertain nanotoxicological effects in other immune cell types as well, such as those that can evoke allergic reactions due to work or environmental exposure to increasingly ubiquitous 2D materials. Basophils, which are involved in atopic skin, airway inflammation, and parasite immunity in the gut and skin (Schwartz et al., 2016). Basophils can synthesize and secrete inflammatory mediators such as histamine or cytokines upon activation of IgE receptor or *via* IgE-independent pathways with chemotactic peptides such as N-formyl-methionyl-leucyl-phenylalanine (fMLP) (Valent and Bettelheim, 1990). Additionally, basophils are also able to augment inflammation by recruiting effector cells, like T helper type 2 cells, eosinophils, and inflammatory macrophages, which may exacerbate allergy (Schwartz et al., 2016). Despite being a minor population, blood basophils are important as readouts of allergy and can therefore be used as a source of primary human immune cells to investigate the potential impact of foreign materials.

Currently, MoS_2 and 2D materials in general are produced by both bottom up (growth onto a substrate) and top down (exfoliation from bulk counterparts) approaches (Backes et al., 2020; Bonaccorso et al., 2012; Bonaccorso et al., 2016). However, a key requirement for the development of any application relies on the advancement of industrial-scale, inexpensive, reliable production processes, while providing a balance between ease of fabrication and final material quality. Solution-processing offers a simple and cost-effective pathway to fabricate various 2D crystal based photonic devices, presenting huge integration flexibility compared to conventional methods. In this context, the liquid phase exfoliation (LPE) approach offers a simple and cost-effective pathway toward industrialization, due to low cost, quality, and large-scale production (Kg scale) The LPE process is carried out both in organic solvents (*e.g.*, *N*-methyl pyrrolidone or alcohols) or in aqueous solution with the aid of stabilizers (*i.e.*, surfactants, polymers) (Bonaccorso et al., 2016). Surfactants, like sodium deoxycholate, are added during the LPE to provide the steric hindrance, preventing the exfoliated flakes from re-stacking (Sun et al., 2017). Similarly, more biologically inert compounds such as glycine can also be used as exfoliating agents for 2D materials during mechanochemical exfoliation (Gonzalez et al., 2020).

In this paper, we compare 2D MoS_2 from two different industrial sources to test their effects on primary human blood basophils to understand their potential impact on allergy. In this regard, BeDimensional (BD) manufactures MoS_2 using the anionic sodium deoxycholate as an exfoliating agent under high piston pressure. At the same time, the second company, Biograph Solutions (BS), produces MoS_2 using non-ionic glycine as an exfoliating agent during ball-milling as a form of mechanochemical preparation. Sodium deoxycholate is already widely used in the production of MoS_2 (Howe et al., 2015), and it can act as both drug dispersing and permeation-modifying agents despite reported toxicity that manifests in supraphysiological concentrations (Pavlović et al., 2018). A sodium deoxycholate control was included in our biological experiments to exclude potential side effects. As glycine is a natural amino acid and it was present only in traces in the final material, there was no need to include it as a control. Flow cytometry was established to measure basophilic surface membrane markers such as CD63 and CD203c in allergy diagnosis (Bridts et al., 2014), with cytokine ELISA complementing the data.

2. Materials and methods

2.1. Preparation of materials

For BeDimensional, natural MoS_2 crystals (size ~1 cm^2) from Smart Elements were used as starting material. The crystals were crushed using a mortar. Crystallites (1 wt%) were then mixed with sterile 0.5 L MilliQ® water and sodium deoxycholate (Sigma Aldrich) at 0.1 wt%. Exfoliation was performed using a high-pressure homogeniser, as previously reported (Del Rio Castillo et al., 2018). With a piston pressure of 250 MPa for exfoliation, five piston passes were performed through a nozzle of 0.1 mm diameter. The obtained dispersion is centrifuged in a Hettich Rotina 420R at 15000*g*. The supernatant is collected, obtaining BD MoS_2 flakes.

For Biograph Solutions, 2D MoS_2 was synthesized through a mechanochemical method starting with bulk MoS_2 as precursor material and glycine as an exfoliating agent (all from Sigma Aldrich) as previously reported (Gonzalez et al., 2020). Briefly, 75 mg of MoS_2 in bulk and 2.5 g of glycine were placed in a 250 mL stainless steel jar containing 15 stainless steel balls (2 cm in diameter each). The materials were treated using a planetary ball-milling machine (Retsch pm100) for 15 min at 250 rpm, followed by dispersion in 100 mL of water and further dialysis heating at 70 °C (with five water changes every 90 min, and one overnight) to remove the excess of glycine. Finally, the dispersions were lyophilized at −80 °C at a pressure of 0.005 bar to obtain the material in powder form. 2D MoS_2 powder was then heated in a furnace under an N_2 atmosphere, using a 10 °C/ min ramp up to 129 °C, followed by a 60 min isothermal and finally, a cooling ramp (2 °C/ min until 25 °C) as previously published (Fusco et al., 2020). Sodium deoxycholate (Sigma) was filter-sterilized and used at a final concentration of 30 μg/mL. Sodium molybdate dihydrate (Sigma) was filter-sterilized and used at a final concentration of 75 μg/mL. All materials tested were endotoxin-free in primary human macrophages compared to LPS controls (Mukherjee et al., 2016). In order to avoid possible spontaneous transformation of MoS_2 in solution (Kurapati et al., 2017b; Marks et al., 2020), the dispersions were stored in the dark and under argon. Regular controls using XPS were done to follow the eventual oxidation of the material alongside cellular experiments."

2.2. Transmission electron microscopy

Transmission electron microscopy (TEM) was used to verify the quality of the sheets and to measure the average lateral size. Morphological analyses on both materials were performed using a transmission electron microscope (Hitachi 7500, Hitachi High Technologies Corporation, Tokyo, Japan). MoS_2 samples were prepared by drop-casting the dispersion onto ultrathin C-film on Formvar carbon 300 mesh Cu grids (Electron Microscopy Sciences). The samples were diluted to 15 μg/ mL in sterile water.

2.3. Atomic force microscopy

The dispersions were diluted at 1:30. One hundreds μL of the dilutions were drop-cast onto mica wafers previously cleaved and cleaned, and dried at 50 °C. Atomic force microscopy images were acquired with a Bruker Innova® AFM in tapping mode using silicon probes (frequency = 300 kHz, spring constant = 40 Nm^{-1}). Thickness statistics were performed by measuring >40 flakes from the AFM images. Statistical analyses are fitted with log-normal distributions. Statistical analysis was performed in WSxM Beta 4.0 software.

2.4. Raman spectroscopy

BeDimensional dispersions were drop-cast onto a Si wafer (LDB Technologies Ltd.) covered with 300 nm thermally grown SiO_2. Bulk materials were analyzed as received. Raman measurements were carried out by a Renishaw inVia microspectrophotometer using a 50× objective (numerical aperture 0.75), a laser with a wavelength of 514.5 nm with an incident power of ~5 mW under ambient conditions. >100 points per sample were measured to perform the statistical analysis.

For Biograph Solutions, Raman analyses were recorded under ambient conditions using 30 points in powder samples on an inVia Renishaw microspectrophotometer using a 50× objective and a 532 nm point-based laser and a power density below 1 mW/μm^2.

2.5. X-ray photoelectron spectroscopy

X-ray photoelectron spectroscopy (XPS) analyses were performed on a Thermo Scientific K-Alpha X-ray photoelectron spectrometer with a basic chamber pressure of 10^{-8} to 10^{-9} bar with an anode using Al Kα radiation ($h\nu = 1486.6$ eV). The samples were analyzed as powder pressed onto a scotch tape (3MTM EMI Copper Foil Shielding Tape 118). A spot size of 400 μm was used. The survey spectra are displayed as an average of 10 scans with a pass energy of 200.00 eV and a step size of 1 eV. The high-resolution spectra of S 2p and Mo 3d are an average of 20 scans with a pass energy of 50 eV and a step size of 0.1 eV, while the spectra of C1s are an average of 20 scans. For each sample, the analysis was repeated three times. A flood gun was turned on during analysis. For data analysis, the software casaXPS (2.3.18) was used. A Shirley background subtraction was applied. A line-shape 80% Gaussian/20% Lorentzian [GL(20)] was selected for all peaks. Mo 3d spectra were deconvoluted in Mo 3d (229.35–229.75 eV for $3d_{5/2}$ and 232.55–232.95 eV for $3d_{3/2}$), MoO_3 (232.85–233.25 eV for $3d_{5/2}$ and 235.85–236.45 eV for $3d_{3/2}$) and overlapped S 2 s. The full width at half maximum was constrained to be the same for all peaks. For Mo-S-benzoquinone. The S 2p spectra were deconvoluted in S 2p (163.05–163.35 eV for $2d_{1/2}$ and 161.8–162.2 eV for $2p_{3/2}$), S—C (163.8–164.6 eV for $2d_{1/2}$ and 162.6–163.4 eV for $2p_{3/2}$), and S—F (172.0–172.8 eV).

2.6. Zeta potential

Stock solutions of both materials were diluted in Milli-Q water to 0.1 mg/mL for zeta potential measurements. All tests were performed in triplicate at 25 °C with 120 s equilibration time using a Malvern Zetasizer Nano ZS (Malvern Instruments).

2.7. Thermogravimetric analysis

BeDimensional MoS_2 thermogravimetric analysis was performed on a TGA1 Mettler Toledo apparatus from 30 °C to 900 °C with a ramp of 10 °C/min under an N_2 atmosphere with a flow rate of 50 mL/min and platinum pans.

Biograph Solutions MoS_2 analysis was made in a TGA Q50 (TA Instruments) equipment using a ramp of 10 °C/min from 100 °C to 800 °C under an N_2 atmosphere.

2.8. Isolation of primary immune cells

Human peripheral blood basophils were isolated from buffy coats obtained from the French Blood Bank (Etablissement Français du Sang, Strasbourg, France, contract no. ALC/PIL/DIR/AJR/FO/606). The blood samples were from anonymous healthy donors, and they do not require ethical approval. Basophils were directly isolated from peripheral blood mononuclear cells (PBMCs) using a commercial kit (Miltenyi, #130–094-434). Cells were cultured in RPMI (Lonza) supplemented with 10% heat-inactivated fetal bovine serum (FBS) and 1% penicillin/streptomycin. Basophils were characterized as CCR3+, FceRI+ with low CD203c expression, and visualized with an optical microscope using acidic toluidine blue (Fig. S1). Tested materials were added at a low dose (5 μg/mL) and a higher non-toxic dose (50 μg/ mL) in the presence of 10 ng/mL IL-3 (Peprotech) and analyzed 1 or 18 h later in the presence or absence of activators 500 ng/mL anti-IgE (ThermoFisher, #SA5–10259,) or 100 nM fMLP (Merck, #F3506). Cells were cultured in RPMI (Lonza) supplemented with 10% heat-inactivated fetal bovine serum (FBS) and 1% penicillin/streptomycin.

2.9. Flow cytometer analyses

Viability and activation of 18 h MoS_2-treated cells were assessed using flow cytometry (Beckman Coulter Gallios). Cells were washed with 2% FBS in PBS (Flow Cytometry Staining Buffer, FACS Buffer), then stained with the respective antibody mix at 4 °C for 20 min. The anti-human antibodies used to characterize basophils or to measure activation were CCR3-FITC (Biolegend, #310720), FcεRI-FITC (Biolegend, #334608), CD123-PE (BD, #555644), CD203c-PerCP/Cyanine5.5 (Biolegend, #324608), CD63-PE (BD, #353004) and CD69-APC (Miltenyi, #130–112-614). The viability of cells was analyzed by staining with Fixable Viability Dye (eBioscience FVD-eFluor 780, #65–0865-14). Reactive oxygen species (ROS) production was analyzed by staining with CM-H2DCFDA (ThermoFisher Science, #C6827) for 30 min at 37 °C. After staining, cells were washed twice with FACS buffer, then resuspended in fresh FACS buffer and analyzed on the flow cytometer.

2.10. ELISA tests

Secretion of the cytokines IL-6 (BD Opt-EIA #555220), IL-1β (BD Opt-EIA #557953), TNF (BD Opt-EIA #555212), IL-13 (Biolegend #435207), IL-4 (BD #430304), GM-CSF (BD #555126) of cells treated with different concentrations of MoS_2 (*i.e.*, 5, 50 μg/mL), were assayed with ELISA kits according to the manufacturer's instructions. In short, polyvinyl microtiter 96-well plates (Falcon) were coated overnight at 4 °C with 50 μL/well of purified capture antibodies diluted in coating buffer (carbonate/bicarbonate buffer 0.05 M, pH 9.6). After washing with PBS containing 0.05% Tween (PBS-T), a blocking step was performed by adding 5% FBS in PBS (100 μL/well) for 1 h at room temperature. After washing thrice with PBS-T, 50 μL of culture supernatants from the treated cells were added to the respective wells for 2 h at room temperature, along with a respective series of standards as provided in the kits. The plates were then washed five times with PBS-T. Secondary antibodies as provided in the kit were added together with horseradish peroxidase (HRP) reagent and incubated for 1 h at room temperature. Then, the plates were washed five times with PBS-T, and the presence of cytokines in the tested supernatants was visualized by adding tetramethylbenzidine in the presence of H_2O_2. The resulting absorbance was measured at 450 nm after stopping the reaction with 2 N H_2SO_4, after 15 min.

2.11. Statistical analysis

Experiments were conducted at least three times and the data were processed by GraphPad Prism 7. Results are expressed as mean ± standard deviations (SD). One-way ANOVA followed by Bonferroni's test was performed to determine the statistical differences among samples *versus* control untreated cells (*, $p \leq 0.05$; **, $p \leq 0.01$, ***, $p \leq 0.001$).

3. Results

3.1. Preparation and characterization of 2D MoS_2 materials

2D MoS_2 was provided by the commercial companies BeDimensional and Biograph Solutions. For BD, bulk MoS_2 was directly exfoliated by the LPE process in the presence of 50% sodium deoxycholate to obtain a

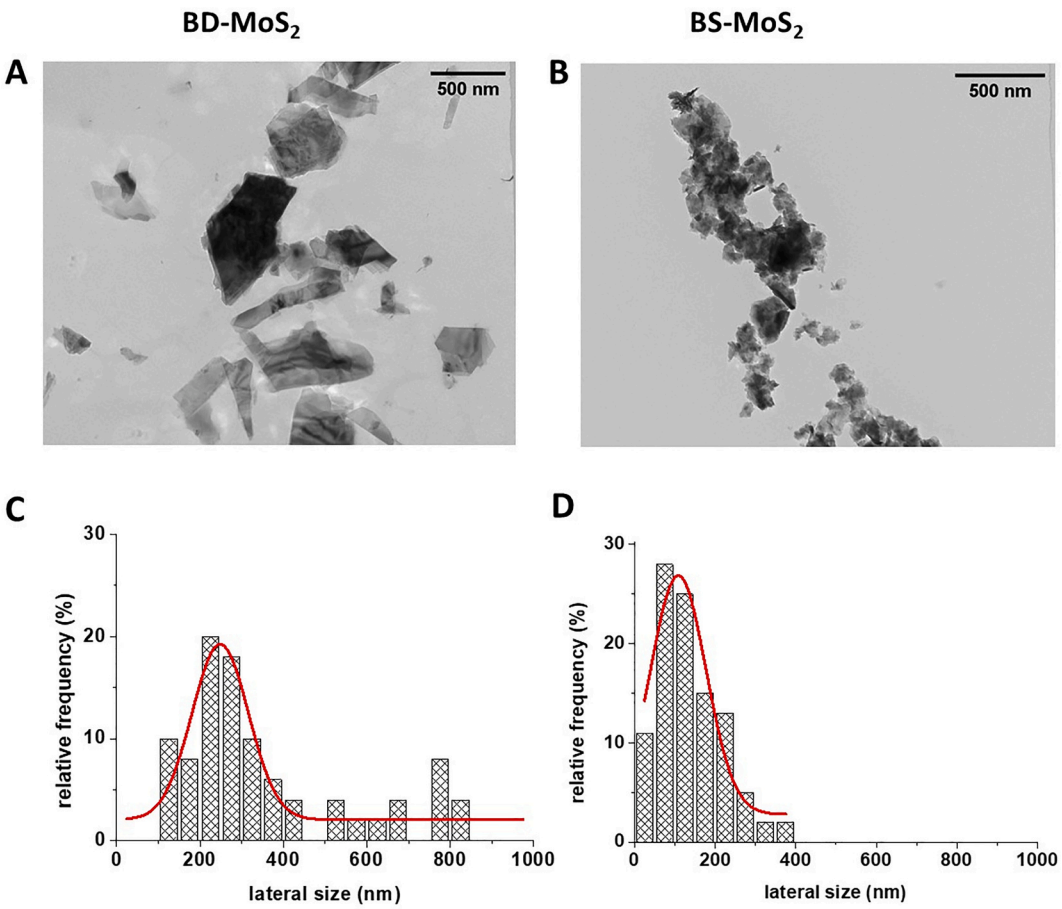

Fig. 1. Materials characterization. TEM of (A) BD-MoS_2 (50000×). TEM of (B) BS-MoS_2 (80000×). Lateral size distribution of (C) BD-MoS_2 calculated from TEM images by measuring 50 sheets (D) BS-MoS_2 calculated from TEM or HR-TEM images by measuring 101 sheets.

dispersion of MoS_2 in water. For BS, MoS_2 was prepared by ball milling bulk material in the presence of glycine, extracted and isolated as a solid (see Experimental section for details). TGA analysis quantifies the amount of the surfactant used to stabilize both MoS_2. The BD-MoS_2 contained ~50 wt% of sodium deoxycholate. (Fig. S2A), while BS-MoS_2 sample contained <3 wt% of glycine (Fig. S2B).

Stocks of MoS_2 dispersions at 1 mg/mL in sterile water were then prepared for the cellular experiments. The colloidal stability in water was verified by measuring the ζ-potentials corresponding to −45.86 +/− 11.98 and − 31.41 +/− 6.02 mV for BD- and BS-MoS_2, respectively, similar to typical values reported in the literature (Forsberg et al., 2016).

Both materials were further characterized by TEM (Fig. 1A, B). In the case of BD-MoS_2, TEM micrographs showed single and few-layer sheets with a lateral size mode of 240 nm and a lognormal standard deviation of 0.53 (Fig. 1C). The lateral size distribution was calculated from TEM images by measuring >200 flakes, showing values ranging between 100 and 850 nm, with a few sheets reaching a maximum of 800 nm. The lateral size mode of BS MoS_2 is 132 nm with a lognormal standard deviation of 0.75, with values ranging between 25 and 375 nm. These values were obtained by measuring >100 flakes. We also measured the thickness of the flakes by AFM, obtaining the values of 1.2 nm and 3.2 nm for BD- and BS-MoS_2 samples, respectively (Fig. S3).

To better understand the structural and surface properties of the materials, Raman and XPS measurements were carried out. Raman spectrum of BD-MoS_2 displayed the two characteristic bands at 380 and 406 cm^{-1}, corresponding to the peaks of in-plane E^1_{2g} and out-of-plane A_{1g} vibration modes of the hexagonal MoS_2 crystal, respectively (Fig. 2A). In the case of BS-MoS_2, the same two characteristic bands appeared slightly shifted at 379 and 405 cm^{-1} (Fig. 2B) (Shahzad et al., 2017).

Finally, the materials were characterized by XPS. From the survey spectrum (Fig. 2C), Mo, S, C, O and Na were identified in the material from BD. Since BD-MoS_2 was obtained by exfoliation with sodium deoxycholate, the adsorption of surfactant to the surface of the material led to high intensity of emission for the C and O, hampering a correct quantification of their amount, as the presence of ubiquitous carbon contaminations on the sample, occurring during air exposure, complicated the calculation of the amount of sodium deoxycholate based on carbon and oxygen elements. It was also not possible to rely on the intensity of sodium because sodium can exchange in solution, leading to the removal of part of Na^+ during purification steps. Therefore, we relied on the values obtained by TGA (see above). In the case of BS-MoS_2, only C, O, Mo and S were observed (Fig. 2F). Again, we could not calculate the quantity of glycine from the survey data. Indeed, as mentioned above, ubiquitous carbon contamination hinders the actual contribution of C and O elements. In addition, it was not possible to identify the N 1 s orbital because it overlaps with the Mo 3p peak. In parallel, we recorded the high-resolution spectra of Mo and S for both materials (Fig. 2D-H). The deconvolution of Mo 3d spectra revealed five different peaks. While the peak at 226.8 eV relates to S 2 s orbital, Mo $3d_{5/2}$ and Mo $3d_{3/2}$ at 229.5 and 232.6 eV, respectively, correspond to the binding energies of Mo^{4+} (Fig. 2D, G). A low percentage of oxidized molybdenum was also observed. Indeed, the peaks of Mo $3d_{5/2}$ and Mo $3d_{3/2}$ at 233.2 and 235.8 eV, respectively, are attributed to Mo^{6+} (Fig. 2D, G). Based on the relative intensities of the four Mo peaks, the percentages of Mo^{4+} and Mo^{6+} are 79.5% and 20.5% in BD-MoS_2, respectively, while they are 90.3% and 9.7% in BS-MoS_2. In the high-

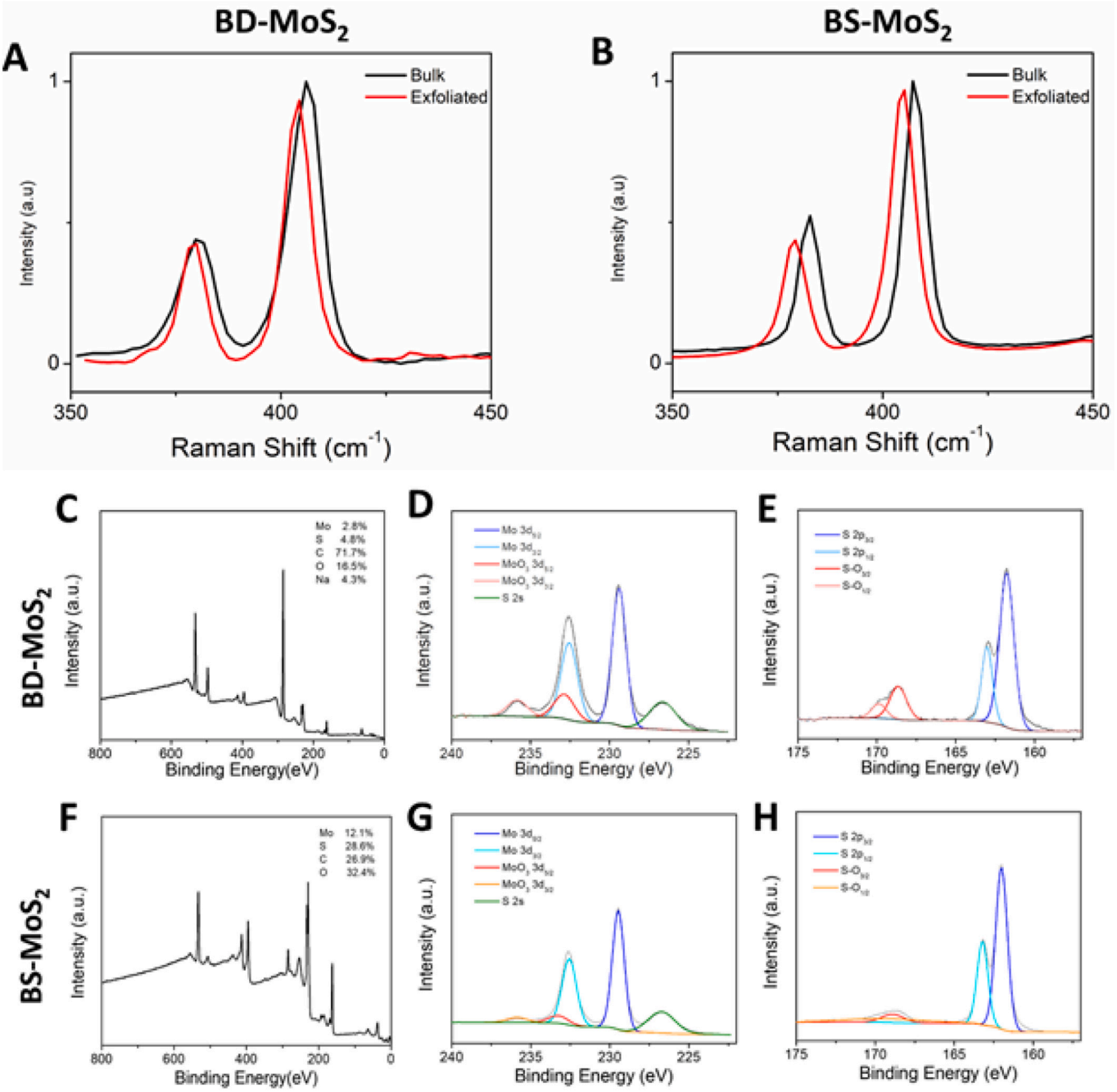

Fig. 2. Materials characterization. Raman spectra of (A) BD-MoS_2 (B) BS-MoS_2. XPS spectra of BD-MoS_2 (C-E) Survey spectra of MoS_2 (C) high-resolution spectra of MoS_2 (D) Mo 3d and S 2p (E). XPS spectra of BS-MoS_2 (F—H) Survey spectra of MoS_2 (F) high-resolution spectra of MoS_2 (G) Mo 3d and S 2p (H).

resolution S 2p spectra, MoS_2 from both companies displayed one doublet corresponding to the binding energies of S $2p_{3/2}$ and S $2p_{1/2}$ centered at 161.9 eV and 163.3 eV, respectively, and one doublet for S—O with the S-$O_{3/2}$ centered at 168.6 eV and S-$O_{1/2}$ located at 170.1 eV (Fig. 2E, H). The second doublet indicates again that the materials were slightly oxidized during their preparation, likely due to oxygen from the air.

3.2. Basophil viability and activation

Basophils were isolated from healthy human donor peripheral blood mononuclear cells using a commercial kit and characterized as detailed in the Methods section (Fig. S1). Both MoS_2 materials at doses of 5 and 50 μg/mL, as similarly used in our previous work comparing the impact of various 2D materials in dendritic cells (Lin et al., 2022) did not show detrimental effects on viability at 1 or 18 h (Fig. 3A, B), even in the presence of basophil activators anti-IgE or fMLP, although deoxycholate, showed a significant decrease of viable cells. These non-toxic doses were also within the range of published data from other labs (Chen et al., 2018a; Nouzil et al., 2022). The absence of detrimental effects is in line with previously published data from our group, showing that MoS_2 is minimally toxic in human macrophages with slight alterations in cell stress and inflammatory responses (Lin et al., 2020).

In terms of surface activation markers, the expression of CD63 and CD203c increased by adding anti-IgE or fMLP, as expected, for all treatment conditions (Fig. 3C-3F). A decrease in fMLP-stimulated with 50 μg/mL BD MoS_2 was observed at 18 h, although this effect is not significant (Fig. 3D). Higher CD63 levels were observed for fMLP in

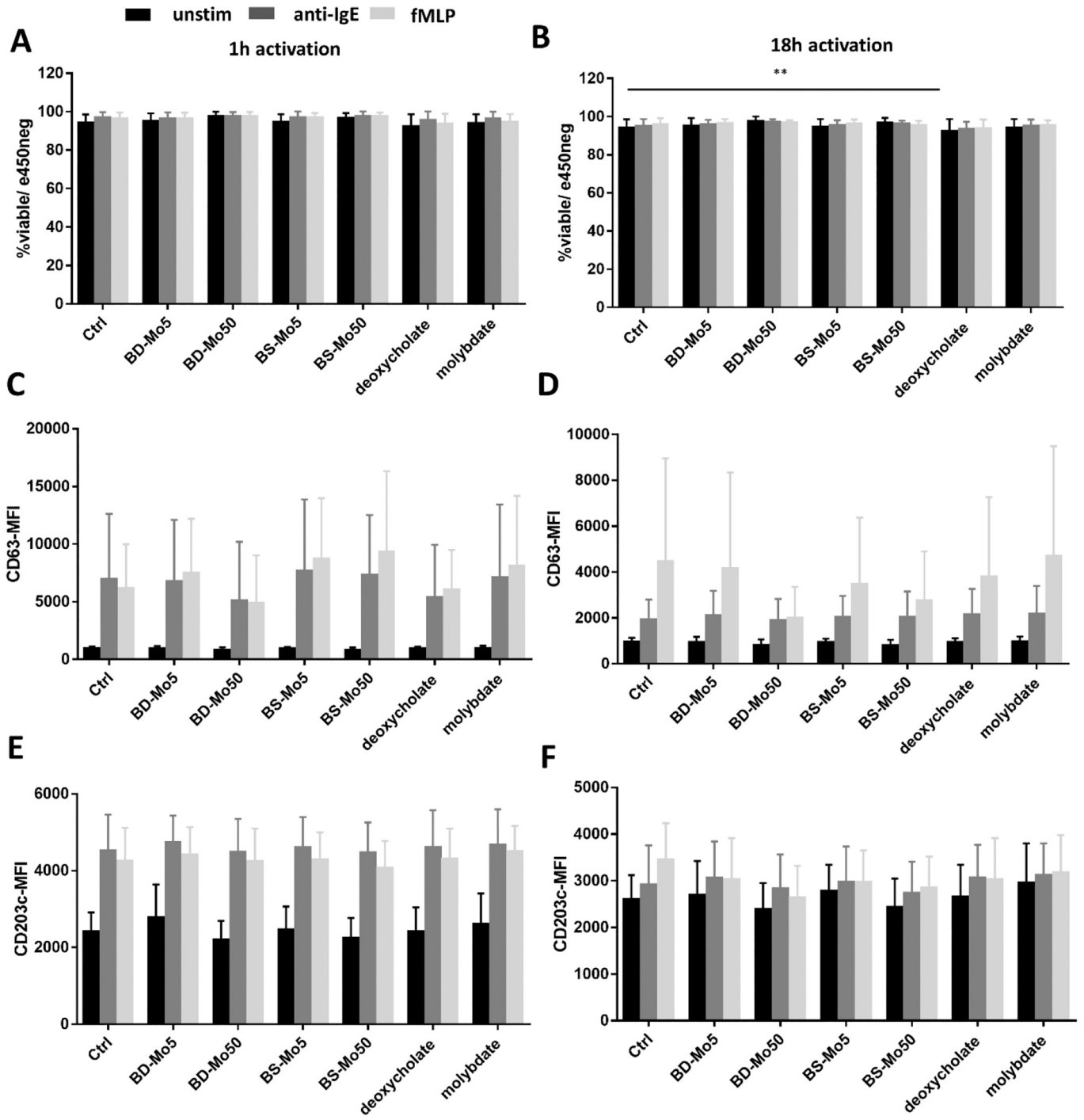

Fig. 3. Materials did not have a detrimental impact on basophil viability and surface markers. Viability following the treatment of basophils with 5, 50 μg/mL BD- or BS-MoS_2 for (A) 1 h (B) 18 h. CD63 expression of basophils treated with 5, 50 μg/mL BD- or BS-MoS_2 for (C) 1 h (D) 18 h. CD203c expression of basophils treated with 5, 50 μg/mL BD- or BS-MoS_2 for (E) 1 h (F) 18 h. All experiments were conducted thrice in triplicate and shown as mean ± SD. $^{*}P < 0.05$; $^{**}P < 0.01$, $^{***}P < 0.001$ by one-way ANOVA with Bonferroni post-tests.

general for all materials at 18 h compared to anti-IgE, but these were not significant too (Fig. 3D). No apparent differences were noted between treatment conditions for CD203c at 1 or 18 h (Fig. 3E, F). No changes were observed in the expression of the long-term activation marker CD69 between all treatment conditions at 18 h, despite a slight expected increase of each treatment with anti-IgE or fMLP stimulation (Fig. S4).

3.3. Basophil histamine release and reactive oxygen species production

Basophils are the primary source of inflammatory mediators, such as histamine, in the blood. Secretion of histamine and other products of degranulation can be triggered by anti-IgE or fMLP. Indeed, an increase in histamine was observed upon adding anti-IgE or fMLP (Fig. 4A). The untreated control and low dose 5 μg/mL BD-MoS_2 had inferior baseline histamine release compared to the other treatments. In short, high dose

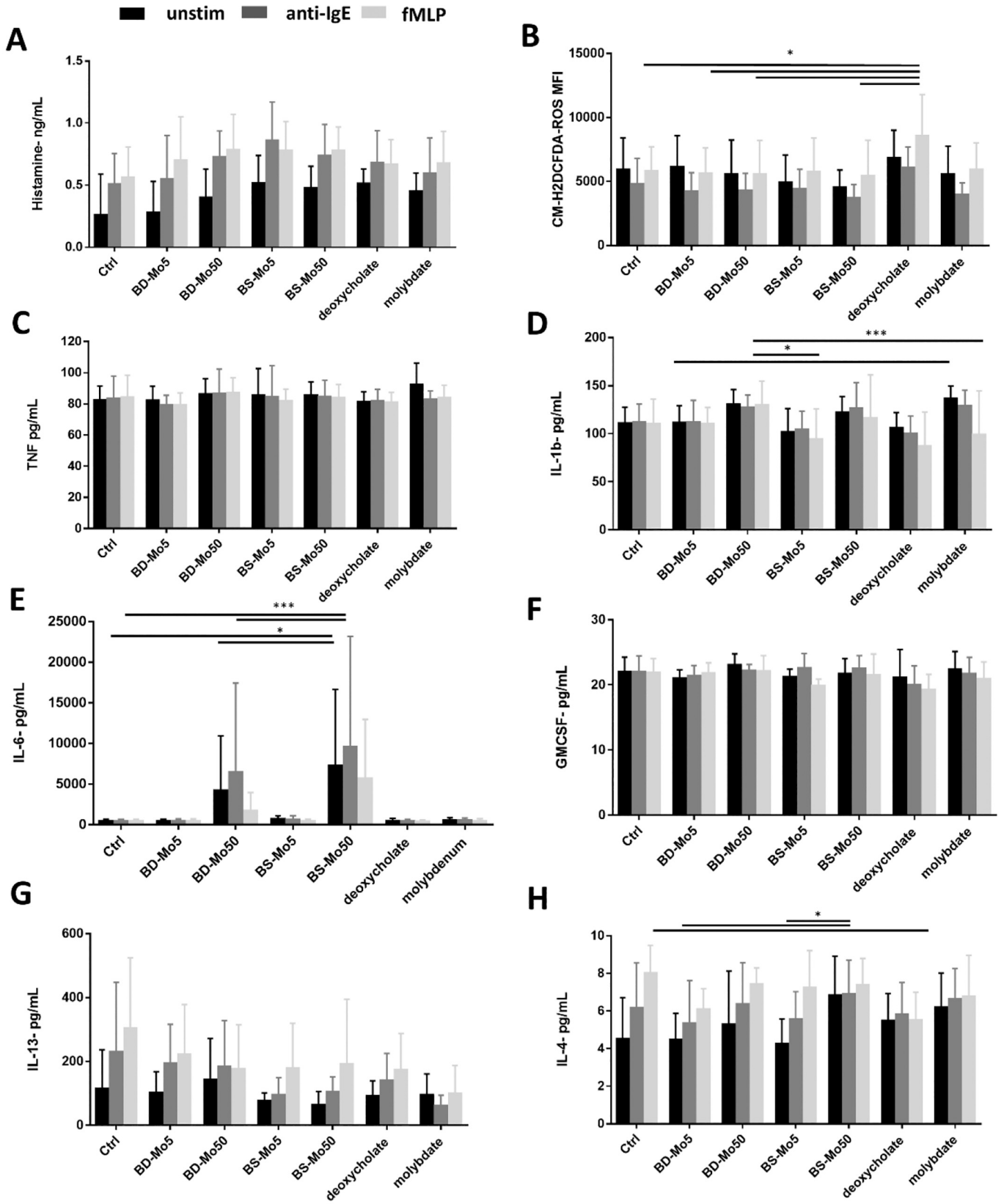

Fig. 4. Materials had minimal impact on basophil histamine, ROS and cytokine production. (A) Histamine and (B) ROS production following the treatment of basophils with 5, 50 μg/mL BD- or BS-MoS_2 for 1 h for histamine and 18 h for ROS. (C) TNF (D) IL-1β (E) IL-6 (F) GM-CSF (G) IL-13 (H) IL-4 expression of basophils treated with 5, 50 μg/mL BD- or BS-MoS_2 for 18 h. All experiments were conducted thrice in triplicate and shown as mean ± SD. *$P < 0.05$; **$P < 0.01$, ***$P < 0.001$ by one-way ANOVA with Bonferroni post-tests.

(50 μg/mL) BD MoS_2 and both doses of BS-MoS_2 had slightly higher histamine release compared to untreated control with or without anti-IgE or fMLP. Interestingly, there was a minor increase in anti-IgE and fMLP-triggered histamine amounts for deoxycholate and molybdate than the other combinations. These effects were, however, not significant.

ROS production has been a hallmark of oxidative stress in many cell types. At 18 h, no change in ROS production was seen in all materials with or without anti-IgE or fMLP stimulation, except for fMLP-stimulated deoxycholate. ROS production of 5 μg/mL and 50 μg/mL BS-MoS_2 was notably but non-significantly lower than the other treatment conditions **(**Fig. 4B**)**.

3.4. Basophil cytokine production

Basophil production of the pro-inflammatory cytokines TNF, IL-1β and IL-6 were investigated after 18 h treatment with both MoS_2 samples. No apparent change in TNF production was observed with all treatment conditions, even in the presence of basophil stimulators anti-IgE and fMLP (Fig. 4C**)**. An increase in IL-1β was seen instead with molybdate in unstimulated basophils compared to untreated, unstimulated basophils, with a decrease seen in contrast upon stimulation with fMLP for molybdate-treated basophils **(**Fig. 4D**)**. High dose 50 μg/mL BD- and BS-MoS_2 also showed an increase in IL-1β in unstimulated and anti-IgE-stimulated basophils compared to the untreated basophils, although this effect was not significant unlike that with molybdate **(**Fig. 4D**)**.

Production of the pro-inflammatory cytokine IL-6 was only observed with both BD- and BS-MoS_2 at 50 μg/mL, with the latter producing a more pronounced increase. For both types of MoS_2, the increase in IL-6 was augmented upon stimulation with anti-IgE. There was no effect with fMLP stimulation for 50 μg/mL BS-MoS_2, while a non-significant increase of IL-6 was seen with 50 μg/mL BD-MoS_2 **(**Fig. 4E**)**. GM-CSF is a cytokine product of activated cells as a result of pathologic or inflammatory conditions (Ushach and Zlotnik, 2016). No effect on GM-CSF was observed with all treatment conditions with or without anti-IgE or fMLP **(**Fig. 4F**)**.

IL-13 is a cytokine implicated in asthma, fibrosis and allergic inflammation (Rael and Lockey, 2011). A non-significant increase in IL-13 upon stimulation with anti-IgE or fMLP was noted, with a greater magnitude of increase with fMLP. Although non-significant, changes were more significant for both doses of non-stimulated BD-MoS_2 than that of BS-MoS_2. No change with anti-IgE or fMLP was seen for molybdate-treated basophils **(**Fig. 4G**)**.

Deoxycholate-treated fMLP-stimulated basophils produced markedly less of the immunoregulatory cytokine IL-4 than the unstimulated and anti-IgE-stimulated deoxycholate-treated basophils. Molybdate-treated and 50 μg/mL BS-MoS_2 had higher IL-4 than the other treatment conditions in unstimulated and anti-IgE-stimulated basophils. Low dose BD-MoS_2 and deoxycholate-treated basophils had non-significantly lower fMLP-stimulated IL-4 production than the other treatment conditions **(**Fig. 4H**)**.

4. Discussion

MoS_2 has been recognised as a viable graphene substitute due to its strength and electrical properties, facile synthesis and rich abundance of natural source material molybdenite. The comparison between the effects of MoS_2 and graphene were previously reviewed by Chondakar et al. (Chodankar et al., 2020). MoS_2 has a band gap, unlike graphene, which makes it suitable for electronic components such as transistors and logic circuits. MoS_2 will thus have great potential to make inroads in a future with many nanobioelectronic applications.

In this study, we have selected two types of MoS_2 samples, prepared by two companies. Despite the different chemical stabilizers and production methods, the size distribution and thickness of both materials are similar, as demonstrated by TEM and AFM. Additionally, Raman spectra for both MoS_2 were similar, confirming the quality of 2D nanosheets (Chen et al., 2018b).

Basophils generally do not take up nanomaterials (Fröhlich, 2015), unlike macrophages and dendritic cells. Therefore, MoS_2 is expected to exert its effect by cellular association. The non-toxicity on basophils (even at 18 h) in the presence or absence of anti-IgE or fMLP demonstrated the safe use of exfoliated MoS_2. Sodium deoxycholate, however, led to decreased viability at 18 h, which meant its use in biological applications should be avoided. Given its character as a cell stress inducer, the viability decrease is expected, influencing multiple cellular pathways such as DNA damage, apoptosis, oxidative and endoplasmic reticulum stress (Crowley et al., 2000). The relatively high amount of deoxycholate used in BD-MoS_2 represents a typical industrially produced material that relies on chemical surfactants to reduce agglomeration. This excess deoxycholate could therefore contribute to toxicity. The results of our study may hopefully motivate the community to use non-toxic alternatives.Apart from a predictable increase of activation markers CD63, CD69 and CD203c compared to untreated unstimulated control, no difference was observed for all treatment conditions. Although commonly used as a basophil activation marker, CD63 has been reported to be more highly variable among individuals than CD203c (Chirumbolo et al., 2009). However, using high dilutions of histamine up to 1×10^{-32} mol/L, the authors showed the inhibition of the CD203c upregulation in human basophils (Chirumbolo et al., 2009). As such, the presence of even a low amount of histamine could have contributed to the no increase of CD203c that we observed for the two MoS_2, which by themselves increased histamine production in basophils as we will discuss below.

The effects of histamine, produced mainly by mast cells and basophils in allergy, are pro-inflammatory and indirectly alter the Th1/Th2 balance. Higher histamine levels were seen with the highest dose (50 μg/mL) of BD- and BS-MoS_2 than with untreated control. The higher levels of histamine seen with BD-MoS_2 were in line with the increase of the basophil activation marker CD63, further hinting at a possible effect of high dose BD-MoS_2 in allergic diseases, although it must be considered that increased ROS production or increased CD203c levels were not present. Previous reports describe contradictory histamine responses in rat basophils with different doses of $ZnCl_2$ and decreased histamine release with ZnO (Feltis et al., 2015). Histamine signaling is mediated by four subsets of histamine receptors, which exert differential effects and may have donor-to-donor variation (Branco et al., 2018). No correlation was found between basophil sensitivity and maximum histamine release (MacGlashan Jr., 1993), which thus makes redundant the need to consider the extent of basophil activation concerning observed histamine levels.

No change in ROS production was observed except for an increase with fMLP-stimulated deoxycholate treated basophils. fMLP had been previously shown to be involved in ROS-signaling pathways in neutrophils (Zhu and He, 2006) and monocytes (Faour et al., 2018). However, no fMLP-mediated effect on ROS production was observed in this study with the other treatment conditions, implying either fMLP had minimal effect on ROS in basophils in the experimental system presented or that molybdate (the common component in all non-deoxycholate or untreated conditions) was able to mediate the increase triggered by fMLP. In support of this, a non-significant decrease in ROS was seen with BS-MoS_2, which does not contain deoxycholate. However, more work needs to be done to establish a definite decreasing effect of ROS by molybdate ions.

Regarding cytokines, no changes were seen with TNF or GM-CSF. Human blood basophils release the pro-inflammatory cytokine TNF in response to IgE activation (Falkencrone et al., 2013), but both MoS_2 did not cause any increase, thereby implying minimal IgE-mediated effects. Basophil-derived TNF has also been shown to enhance the immune response in sepsis (Piliponsky et al., 2019) and could potentially be beneficial if increased, but MoS_2 did not demonstrate this. GM-CSF is a circulating inflammatory cytokine relevant in macrophage maturation

and possibly lymphoid and myeloid communication that can be produced upon activation in many cell types (Hamilton, 2020). Both MoS_2 did not trigger the production of TNF and GM-CSF, thus demonstrating low inflammatory risk.

Th17 cells have been implicated in allergic sensitization and asthma (Zhao et al., 2013) while Th1 cells negatively regulate pro-allergy Th2 cells (Romagnani, 2000). Human basophils have interestingly been postulated to augment not only Th17 but also Th1 responses and have been seen to accumulate in certain Th17-related conditions (Wakahara et al., 2012). IL-6 from bone marrow-derived basophils have been implicated in Th17 response (Yuk et al., 2017). High-dose (50 μg/mL) of BD- and BS-MoS_2 increased IL-6 and IL-1β, while molybdate alone increased IL-1β, an inflammasome-related cytokine. Increased IL-1β production has previously been associated with molybdenum in dental materials (Ozen et al., 2005). MoS_2 has also been reported to increase IL-6 and IL-1β in human bronchial cells (Zapór et al., 2022) and to increase IL-6 in primary human macrophages (Lin et al., 2020), and our data are in agreement with this behavior.

Activated basophils display heterogeneous phenotypes and have distinct subsets expressing IL-4, IL-13 or activation markers (Pellefigues et al., 2021). BD-MoS_2 increased IL-13, but this was not observed using deoxycholate or molybdate in the control conditions. It has been shown that IL-13 is produced in human blood basophils in response to both IgE-mediated and IgE-independent activation, although higher levels are produced during the IgE-independent activation. Interestingly, IL-4, which is located on the same gene cluster as IL-13, has been preferentially expressed over IL-13 in response to IgE-cross-linking (Ochensberger et al., 1996).

High dose (50 μg/mL) of BS-MoS_2 and molybdate increased IL-4 for unstimulated and anti-IgE-stimulated basophils. In contrast, BD-MoS_2 and deoxycholate-treated fMLP-stimulated basophils decreased this cytokine. The pro-inflammatory response of Th2 has been associated with high levels of IL-4 and IL-13 and basophils have been known to be a major source of IL-4, thus their strong link with Th2 polarization (Min et al., 2004). Basophil-derived IL-4 has been shown to contribute to inflammation in a subset of innate lymphoid cells in the asthmatic lung (Motomura et al., 2014). This alludes to the inflammatory potential of BS-MoS_2 and molybdate even in the absence of IgE stimulation.

5. Conclusions

In this study, we have selected two types of MoS2 samples, prepared by two companies. Despite the different chemical stabilizers and production methods, the size distribution and thickness of both materials are similar, as demonstrated by TEM and AFM. Additionally, Raman spectra for both MoS_2 were comparable, confirming the quality of 2D nanosheets (Chen et al., 2018b). We have reported higher histamine production in two commercially available MoS_2 with no impact on surface basophil activation markers, ROS production or cell viability, but having different cytokine production patterns. In summary, IL-6 and IL-1β, but not TNF and GM-CSF, were increased for both MoS_2. IL-6 alone, which had the most prominent increase compared to untreated control, demonstrated the possibility that much higher doses of MoS_2 cause inflammation regardless of production method. BS-MoS_2 increased IL-4 while BD-MoS_2 decreased IL-4 and increased IL-13. Molybdate ions alone had minimal effects, only increasing IL-1β and IL-4. Deoxycholate on its own decreased long-term viability and increased ROS upon basophil activation. These results ascertain the safety of MoS_2 in human basophils, alluding to low inflammatory potential.

The comparison of two different industrially produced MoS_2 samples in primary human blood basophils has demonstrated different effects. This experimental comparison will hopefully guide downstream user's dependent on product reliability with a better understanding of how different components such as surfactants or exfoliating agents used in the production of industrial 2D materials such as MoS_2 can result in different biological effects. Therefore, it is imperative to investigate experimentally similar 2D materials obtained from different production methods.

Credit author statement

H. L. designed, performed and analyzed the biological experiments, and wrote the first draft; A. E. d. R. C., V. J. G., J. K. P. and L. J. prepared and characterized the materials; F. B. and E. V. supervised the prepration of the materials; A. B. led the study and supervised the work. All authors discussed the results, read, commented, and corrected the manuscript.

Declaration of Competing Interest

The authors declare that they have no known competing financial interests or personal relationships that could have appeared to influence the work reported in this paper.

Data availability

Data will be made available on request.

Acknowledgements

The authors gratefully acknowledge the financial support from the EU Graphene Flagship (project no. 881603). This work was supported by the Interdisciplinary Thematic Institute SysChem *via* IdEx Unistra (ANR-10-IDEX-0002) within the program Investissement d'Avenir. We wish to acknowledge the Centre National de la Recherche Scientifique (CNRS) and the International Center for Frontier Research in Chemistry (icFRC). The authors wish to thank Shi Guo and Yilin He for recording TGA and XPS, and Cathy Royer from the "Plateforme Imagerie In Vitro de l'ITI Neurostra", CNRS UAR 3156, University of Strasbourg (Strasbourg, France), for TEM analyses.

Appendix A. Supplementary data

Supplementary data to this article can be found online at https://doi.org/10.1016/j.impact.2023.100451.

References

ATSDR, Apr 2017. US Agency for Toxic Substances and Disease Registry. Toxicological Profile for Molybdenum. Version. [accessed 7 Apr 2020]. https://www.atsdr.cdc.gov/ToxProfiles/tp212.pdf.

Backes, C., Abdelkader, A.M., Alonso, C., Andrieux-Ledier, A., Arenal, R., Azpeitia, J., et al., 2020. Production and processing of graphene and related materials. 2D Mat. 7, 022001 https://doi.org/10.1088/2053-1583/ab1e0a.

Bonaccorso, F., Lombardo, A., Hasan, T., Sun, Z., Colombo, L., Ferrari, A.C., 2012. Production and processing of graphene and 2D crystals. Mater. Today 15, 564–589. https://doi.org/10.1016/S1369-7021(13)70014-2.

Bonaccorso, F., Bartolotta, A., Coleman, J.N., Backes, C., 2016. 2D-crystal-based functional inks. Adv. Mater. 28, 6136–6166. https://doi.org/10.1002/adma.201506410.

Branco, A.C.C.C., Yoshikawa, F.S.Y., Pietrobon, A.J., Sato, M.N., 2018. Role of histamine in modulating the immune response and inflammation. Mediat. Inflamm. 2018, 9524075. https://doi.org/10.1155/2018/9524075.

Bridts, C.H., Sabato, V., Mertens, C., Hagendorens, M.M., De Clerck, L.S., Ebo, D.G., 2014. Flow cytometric allergy diagnosis: basophil activation techniques. Methods Mol. Biol. 1192, 147–159. https://doi.org/10.1007/978-1-0716-0696-4_15.

Cao, M., Cai, R., Zhao, L., Guo, M., Wang, L., Wang, Y., Zhang, L., Wang, X., Yao, H., Xie, C., Cong, Y., Guan, Y., Tao, X., Wang, Y., Xu, S., Liu, Y., Zhao, Y., Chen, C., 2021. Molybdenum derived from nanomaterials incorporates into molybdenum enzymes and affects their activities in vivo. Nat. Nanotechnol. 16, 708–716. https://doi.org/10.1038/s41565-021-00856-w.

Capasso, A., Matteocci, F., Najafi, L., Prato, M., Buha, J., Cinà, L., Pellegrini, V., Di Carlo, A., Bonaccorso, F., 2016. Few-layer MoS_2 flakes as active buffer layer for stable perovskite solar cells. Adv. Energy Mater. 6, 1600920. https://doi.org/10.1002/aenm.201600920.

Chen, W., Qi, W., Lu, W., Chaudhury, N.R., Yuan, J., Qin, L., Lou, J., 2018a. Direct assessment of the toxicity of molybdenum disulfide atomically thin film and microparticles via cytotoxicity and patch testing. Small 14 (12), e1702600. https://doi.org/10.1002/smll.201702600.

Chen, W., Qi, W., Lu, W., Roy Chaudhury, N., Yuan, J., Qin, L., Lou, J., 2018b. Direct assessment of the toxicity of molybdenum disulfide atomically thin film and microparticles via cytotoxicity and patch testing, 14, e1702600. https://doi.org/10.1002/smll.201702600.

Chirumbolo, S., Brizzi, M., Ortolani, R., Vella, A., Bellavite, P., 2009. Inhibition of CD203c membrane up-regulation in human basophils by high dilutions of histamine: a controlled replication study. Inflamm. Res. 58, 755–764. https://doi.org/10.1007/s00011-009-0044-4.

Chodankar, N.R., Nanjundan, A.K., Losic, D., Dubal, D.P., Baek, J.B., 2020. Graphene and molybdenum disulphide hybrids for energy applications: an update. Mat. Today Adv. 6, 100053 https://doi.org/10.1016/j.mtadv.2019.100053.

Crowley, C.L., Payne, C.M., Bernstein, H., Bernstein, C., Roe, D., 2000. The NAD+ precursors, nicotinic acid and nicotinamide protect cells against apoptosis induced by a multiple stress inducer, deoxycholate. Cell Death Differ. 7, 314–326. https://doi.org/10.1038/sj.cdd.4400658.

Del Rio Castillo, A.E., Pellegrini, V., Ansaldo, A., Ricciardella, F., Sun, H., Marasco, L., Buha, J., Dang, Z., Gagliani, L., Lago, E., Curreli, N., Gentiluomo, S., Palazon, F., Prato, M., Oropesa-Nuñez, R., Toth, P.S., Mantero, E., Crugliano, M., Gamucci, A., Tomadin, A., Polinia, M., Bonaccorso, F., 2018. High-yield production of 2D crystals by wet-jet milling. Mater. Horiz. 5, 890–904. https://doi.org/10.1039/C8MH00487K.

Falkencrone, S., Poulsen, L.K., Bindslev-Jensen, C., Woetmann, A., Odum, N., Poulsen, B. C., Blom, L., Jensen, B.M., Gibbs, B.F., Yasinska, I.M., Sumbayev, V.V., Skov, P.S., 2013. IgE-mediated basophil tumour necrosis factor alpha induces matrix metalloproteinase-9 from monocytes. Allergy 68, 614–620. https://doi.org/10.1111/all.12143.

Faour, W.H., Fayyad-Kazan, H., El Zein, N., 2018. fMLP-dependent activation of Akt and ERK1/2 through ROS/Rho A pathways is mediated through restricted activation of the FPRL1 (FPR2) receptor. Inflamm. Res. 67, 711–722. https://doi.org/10.1007/s00011-018-1163-6.

Federmann, M., Morell, B., Graetz, G., Wyss, M., Elsner, P., von Thiessen, R., Wüthrich, B., Grob, D., 1994. Hypersensitivity to molybdenum as a possible trigger of ANA-negative systemic lupus erythematosus. Ann. Rheum. Dis. 53, 403–405. https://doi.org/10.1136/ard.53.6.403.

Feltis, B.N., Elbaz, A., Wright, P.F.A., Mackay, G.A., Turney, T.W., Lopata, A.L., 2015. Characterizing the inhibitory action of zinc oxide nanoparticles on allergic-type mast cell activation. Mol. Immunol. 66, 139–146. https://doi.org/10.1016/j.molimm.2015.02.021.

Forsberg, V., Zhang, R., Bäckström, J., Dahlström, C., Andres, B., Norgren, M., Andersson, M., Hummelgård, M., Olin, H., 2016. Exfoliated MoS_2 in water without additives. PLoS One 11, e0154522. https://doi.org/10.1371/journal.pone.0154522.

Fröhlich, E., 2015. Value of phagocyte function screening for immunotoxicity of nanoparticles in vivo. Int. J. Nanomedicine 10, 3761–3778. https://doi.org/10.2147/IJN.S83068.

Fusco, L., Pelin, M., Mukherjee, S., Keshavan, S., Sosab, S., Martín, C., González, V., Vázquez, E., Prato, M., Fadeel, B., Tubaro, A., 2020. Keratinocytes are capable of selectively sensing low amounts of graphene-based materials: implications for cutaneous applications. Carbon 159, 598–610. https://doi.org/10.1016/j.carbon.2019.12.064.

Ge, J., Qi, Z., Zhang, L., Shen, X., Shen, Y., Wang, W., Li, Z., 2020. Label-free and enzyme-free detection of microRNA based on a hybridization chain reaction with hemin/G-quadruplex enzymatic catalysis-induced MoS_2 quantum dots via the inner filter effect. Nanoscale. 12, 808–814. https://doi.org/10.1039/c9nr08154b.

Gonzalez, V.J., Rodrıguez, A.M., Payo, I., Vazquez, E., 2020. Mechanochemical preparation of piezoelectric nanomaterials: BN, MoS_2 and WS_2 2D materials and their glycine-cocrystals. Nanoscale Horiz. 5, 331–335. https://doi.org/10.1039/C9NH00494G.

Hamilton, J.A., 2020. GM-CSF in inflammation. J. Exp. Med. 217, e20190945 https://doi.org/10.1084/jem.20190945.

Han, J.H., Kwak, M., Kim, Y., Cheon, J., 2018. Recent advances in the solution-based preparation of two-dimensional layered transition metal chalcogenide nanostructures. Chem. Rev. 118, 6151–6188. https://doi.org/10.1021/acs.chemrev.8b00264.

Howe, R.C.T., Woodward, R.I., Hu, G., Yang, Z., Kelleher, E.J.R., Hasan, T., 2015. Surfactant-aided exfoliation of molybdenum disulfide for ultrafast pulse generation through edge-state saturable absorption. Phys. Status Solidi B 253, 911–917. https://doi.org/10.1002/pssb.201552304.

Hu, J., Zhang, C., Li, X., Du, X., 2020. An electrochemical sensor based on chalcogenide molybdenum disulfide-gold-silver nanocomposite for detection of hydrogen peroxide released by Cancer cells. Sensors (Basel) 20, 6817. https://doi.org/10.3390/s20236817.

IMA, 2008. International Molybdenum Association. Molybdenum Uses [accessed 7 Apr 2020]. https://www.imoa.info/molybdenum-uses/molybdenum-chemistry-uses/molybdenum-chemistry-uses.php.

Köster, R., Vieluf, D., Kiehn, M., Sommerauer, M., Kähler, J., Baldus, S., Meinertz, T., Hamm, C.W., 2000. Nickel and molybdenum contact allergies in patients with coronary in-stent restenosis. Lancet 356, 1895–1897. https://doi.org/10.1016/S0140-6736(00)03262-1.

Kurapati, R., Muzi, L., de Garibay, A.P.R., Russier, J., Voiry, D., Vacchi, I.A., Chhowalla, M., Bianco, A., 2017a. Enzymatic biodegradability of pristine and functionalized transition metal dichalcogenide MoS_2 nanosheets. Adv. Funct. Mater. 1605176. https://doi.org/10.1002/adfm.201605176.

Kurapati, R., Muzi, L., Ruiz de Garibay, A.P., Russier, J., Voiry, D., Vacchi, I.A., Chhowalla, M., Bianco, A., 2017b. Enzymatic biodegradability of pristine and functionalized transition metal dichalcogenide MoS_2 nanosheets. Adv. Funct. Mater. 27 (7), 1605176. https://doi.org/10.1002/adfm.201605176.

Li, X., Zhu, H., 2015. Two-dimensional MoS2: properties, preparation, and applications. J. Mater. 1, 33–44. https://doi.org/10.1016/j.jmat.2015.03.003.

Lin, H., Ji, D.K., Lucherelli, M.A., Reina, G., Ippolito, S., Samorì, P., Bianco, A., 2020. Comparative effects of graphene and molybdenum disulfide on human macrophage toxicity. Small 16, e2002194. https://doi.org/10.1002/smll.202002194.

Lin, H., Song, Z., Bianco, A., 2021. How macrophages respond to two-dimensional materials: a critical overview focusing on toxicity. J. Environ. Sci. Health B 56, 333–356. https://doi.org/10.1080/03601234.2021.1885262.

Lin, H., Peng, S., Guo, S., Ma, B., Lucherelli, M.A., Royer, C., Ippolito, S., Samorì, P., Bianco, A., 2022. 2D materials and primary human dendritic cells: a comparative cytotoxicity study, 18, e2107652. https://doi.org/10.1002/smll.202107652.

MacGlashan Jr., D.W., 1993. Releasability of human basophils: cellular sensitivity and maximal histamine release are independent variables. J. Allergy Clin. Immunol. 91, 605–615. https://doi.org/10.1016/0091-6749(93)90266-i.

Marks, R., Schranck, A., Stillwell, R., Doudrick, K., 2020. Stability of 2H- and 1T-MoS_2 in the presence of aqueous oxidants and its protection by a carbon shell. RSC Adv. 10 (16), 9324–9334. https://doi.org/10.1039/d0ra00788a.

Min, B., Prout, M., Hu-Li, J., Zhu, J., Jankovic, D., Morgan, E.S., Urban Jr., J.F., Dvorak, A.M., Finkelman, F.D., LeGros, G., Paul, W.E., 2004. Basophils produce IL-4 and accumulate in tissues after infection with a Th2-inducing parasite. J. Exp. Med. 200, 507–517. https://doi.org/10.1084/jem.20040590.

Motomura, Y., Morita, H., Moro, K., Nakae, S., Artis, D., Endo, T.A., Kuroki, Y., Ohara, O., Koyasu, S., Kubo, M., 2014. Basophil-derived interleukin-4 controls the function of natural helper cells, a member of ILC2s, in lung inflammation. Immunity 40, 758–771. https://doi.org/10.1016/j.immuni.2014.04.013.

Mukherjee, S.P., Lozano, N., Kucki, M., Del Rio-Castillo, A.E., Newman, L., Vázquez, E., Kostarelos, K., Wick, P., Fadeel, B., 2016. Detection of endotoxin contamination of graphene based materials using the TNF-α expression test and guidelines for endotoxin-free graphene oxide production. PLoS One 11, e0166816. https://doi.org/10.1371/journal.pone.0166816.

Najafi, L., Bellani, S., Martín-García, B., Oropesa-Nuñez, R., Del Rio Castillo, A.E., Prato, M., Moreels, I., Bonaccorso, F., 2017. Solution-processed hybrid graphene flake/2H-MoS2 quantum dot Heterostructures for efficient electrochemical hydrogen evolution. Chem. Mater. 29, 5782–5786. https://doi.org/10.1021/acs.chemmater.7b01897.

Nouzil, I., Eltaggaz, A., Pervaiz, S., Deiab, I., 2022. Toxicity analysis of nano-minimum quantity lubrication machining—a review. Lubricants 10 (8), 176. https://doi.org/10.3390/lubricants10080176.

Ochensberger, B., Daepp, G.C., Rihs, S., Dahinden, C.A., 1996. Human blood basophils produce Interleukin-13 in response to IgE-receptor-dependent and -independent activation. Blood. 88, 3028–3037. https://doi.org/10.1182/blood.V88.8.3028.bloodjournal8883028.

Ozen, J., Atay, A., Beydemir, B., Serdar, M.A., Ural, A.U., Dalkiz, M., Soysal, Y., 2005. In vitro IL-1beta release from gingival fibroblasts in response to pure metals, dental alloys and ceramic. J. Oral Rehabil. 32, 511–517. https://doi.org/10.1111/j.1365-2842.2005.01457.x.

Pavlović, N., Goločorbin-Kon, S., Đanić, M., Stanimirov, B., Al-Salami, H., Stankov, K., Mikov, M., 2018. Bile acids and their derivatives as potential modifiers of drug release and pharmacokinetic profiles. Front. Pharmacol. 9, 1283. https://doi.org/10.3389/fphar.2018.01283.

Pellefigues, C., Mehta, P., Chappell, S., Yumnam, B., Old, S., Camberis, M., LeGros, G., 2021. Diverse innate stimuli activate basophils through pathways involving Syk and IκB kinases. Proc. Natl. Acad. Sci. U. S. A. 118, e2019524118 https://doi.org/10.1073/pnas.2019524118.

Piliponsky, A.M., Shubin, N.J., Lahiri, A.K., Truong, M., Clauson, K., Niino, A.L., Tsuha, S.A., Nedospasov, H., Karasuyama, L.L., Reber, M., Tsai, K., Mukai, S.J. Galli, 2019. Basophil-derived tumor necrosis factor can enhance survival in a sepsis model in mice. Nat. Immunol. 20, 129–140. https://doi.org/10.1038/s41590-018-0288-7.

Rael, E.F., Lockey, R.F., 2011. Interleukin-13 signaling and its role in asthma. World Allerg. Organ J. 4, 54–64. https://doi.org/10.1097/WOX.0b013e31821188e0.

Romagnani, S., 2000. T-cell subsets (Th1 versus Th2). Ann. Allergy Asthma Immunol. 85, 9–18. https://doi.org/10.1016/S1081-1206(10)62426-X.

Schwartz, C., Eberle, J.U., Voehringer, D., 2016. Basophils in inflammation. Eur. J. Pharmacol. 778, 90–95. https://doi.org/10.1016/j.ejphar.2015.04.049.

Shahzad, R., Kim, T.W., Kang, S., 2017. Effects of temperature and pressure on sulfurization of molybdenum nano-sheets for MoS_2 synthesis. Thin Solid Films 641, 79–86. https://doi.org/10.1016/j.tsf.2016.12.041.

Sun, J., Li, X., Guo, W., Zhao, M., Fan, X., Dong, Y., Xu, C., Deng, J., Fu, Y., 2017. Synthesis methods of two-dimensional MoS_2: a brief review. Crystals 7, 198. https://doi.org/10.3390/mi12030240.

Teo, W.Z., Chng, E.L.K., Sofer, Z., Pumera, M., 2014. Cytotoxicity of exfoliated transition-metal dichalcogenides (MoS_2, WS_2, and Wse_2) is lower than that of graphene and its analogues. Chemistry 20, 9627–9632. https://doi.org/10.1002/chem.201402680.

Ushach, I., Zlotnik, A., 2016. Biological role of granulocyte macrophage colony-stimulating factor (GM-CSF) and macrophage colony-stimulating factor (M-CSF) on cells of the myeloid lineage, 100, 481–489. https://doi.org/10.1189/jlb.3RU0316-144R.

Valent, P., Bettelheim, P., 1990. The human basophil. Crit. Rev. Oncol. Hematol. 10, 327–352. https://doi.org/10.1016/1040-8428(90)90009-h.

Wakahara, K., Baba, N., Van, V.Q., Bégin, P., Rubio, M., Ferraro, P., Panzini, B., Wassef, R., Lahaie, R., Caussignac, Y., Tamaz, R., Richard, C., Soucy, G., Delespesse, G., Sarfati, M., 2012. Human basophils interact with memory T cells to augment Th17 responses. Blood 120, 4761–4771. https://doi.org/10.1182/blood-2012-04-424226.

Yuk, C.M., Park, H.J., Kwon, B., Lah, S.J., Chang, J., Kim, J., Lee, K., Park, S., Hong, S., Lee, S., 2017. Basophil-derived IL-6 regulates Th17 cell differentiation and CD4 T cell immunity. Sci. Rep. 7, 41744. https://doi.org/10.1038/srep41744.

Zapór, L., Chojnacka-Puchta, L., Sawicka, D., Miranowicz-Dzierżawska, K., Skowroń, J., 2022. Cytotoxic and pro-inflammatory effects of molybdenum and tungsten disulphide on human bronchial cells. Nanotechnol. Rev. 11, 1263–1272. https://doi.org/10.1021/es500065z.

Zhao, J., Lloyd, C.M., Noble, A., 2013. Th17 responses in chronic allergic airway inflammation abrogate regulatory T-cell-mediated tolerance and contribute to airway remodeling. Mucosal Immunol. 6, 335–346. https://doi.org/10.1038/mi.2012.76.

Zhao, Y., Wei, C., Chen, X., Liu, J., Yu, Q., Liu, Y., Liu, J., 2019. Drug delivery system based on near-infrared light-responsive molybdenum disulfide Nanosheets controls the high-efficiency release of dexamethasone to inhibit inflammation and treat osteoarthritis. ACS Appl. Mater. Interfaces 11, 11587–11601. https://doi.org/10.1021/acsami.8b20372.

Zhu, L., He, P., 2006. fMLP-stimulated release of reactive oxygen species from adherent leukocytes increases microvessel permeability. Am. J. Physiol. Heart Circ. Physiol. 290, H365–H372. https://doi.org/10.1152/ajpheart.00812.2005.